Trends of the surface relaxations, surface energies, and work functions of the 4*d* transition metals

M. Methfessel, D. Hennig,* and M. Scheffler
Fritz-Haber-Institut der Max-Planck-Gesellschaft, Faradayweg 4-6, D-1000 Berlin 33, Germany
(Received 13 December 1991)

Density-functional-theory calculations of the surface energies, surface relaxations, and work functions for a number of low-index surfaces of the 4*d* transition metals from Y to Ag are presented. The calculations were done for seven-layer slabs using the full-potential linear-muffin-tin-orbital method. Agreement with experimentally obtained results is very good for the cases where experimental data are available. Roughly parabolic behavior is found for the top-layer relaxation and the surface energy across the series. The study of trends makes it possible to extract the relevance of different models and to interpret the results within a simple physical picture. The trend in top-layer relaxation can be understood in a model that combines the effects of the inward electrostatic force due to Smoluchowski smoothing with the directed forces due to the localized *d* bonds. The calculated surface energies can be explained by a bond-cutting model, but only if the change of the bond strength with coordination number is taken into account. We find that popular models that relate the surface energy to quantities such as the cohesive energy are flawed because their estimate of the surface energy erroneously includes contributions of the free-atom spin polarization and orbital structure. Several predictions of the surface dependence of work functions, surface energies, and surface relaxations are given.

I. INTRODUCTION

The relaxation of metal surfaces has been studied by means of low-energy electron diffraction (LEED) which, if the measurements are analyzed by multiple-scattering calculations, enables the determination of the atomic positions at the surface.[1] These studies have demonstrated that the outermost atomic layer of most clean metal surfaces shows an inward relaxation; that is, that the spacing between the top two layers is smaller than the bulk interlayer spacing. The top-layer relaxation is often accompanied by smaller shifts of the second and third layers, which can be directed either inward or outward. As a general rule, the magnitude of the relaxation is larger for rough surfaces than for smooth ones, and in many cases a reconstruction of the surface is also observed. On the theoretical side, a number of models have been devised to explain various features of the observed relaxations. These models focus on different aspects, such as the general tendency of the *sp* electrons to spread smoothly at the surface, the different roles of localized *d* electrons and delocalized *sp* electrons, and the way in which the electronic structure is influenced by the termination of a crystal. The complete explanation for the experimentally found relaxations will be a mixture of some or all of these mechanisms, conceivably together with additional effects which have not been considered yet. At the present time, the relevance of the various models is not yet clear. A similar situation exists for the surface energy: this quantity is difficult to measure directly for solid metals, and numerous models have been presented with the aim of obtaining reliable estimates. A popular approach is to use bond-cutting arguments to relate the surface energy to quantities such as the cohesive energy, but the validity of this assumption has not been tested. It is at this point that a useful contribution can be made by *ab initio* total-energy calculations based on density-functional theory (DFT) together with the local-density approximation (LDA) for the exchange-correlation functional.[2,3] This approach has been shown to give reliable results for the ground-state geometry of a wide variety of systems in the bulk as well as for molecules; in the past few years, surfaces have also been considered. The single-particle wave functions, the charge density, and different contributions to the total energy are all accessible, so that it should be possible to extract the dominant effects which influence the surface relaxation and the surface energy. However, previous *ab initio* calculations for metal surface relaxations[4–8] have used a variety of different calculational techniques and have focused on one or two systems at a time, typically different surfaces of the same metal or two metals which are neighbors in the periodic table. While many useful results have been obtained, at the present time no systematic trend studies using the local-density technique have been performed to the author's knowledge, for metal surfaces.

To fill this gap, we present in this paper calculations for various surfaces of the nine 4*d* transition metals from Y to Ag. The series exemplifies the filling of the bonding-antibonding *d* states, but also includes Ag for which the *d* band is filled and lies about 3 eV below the Fermi energy, so that the *sp* electrons are expected to dominate. The series also includes the Pd(100) and Rh(100) surfaces, for which exceptional *outward* relaxations of, respectively, $3.0\%\pm1.5\%$ (Ref. 9) and $0.5\%\pm2\%$ (Ref. 10) have been deduced from LEED. For consistency, all nine metals were first assumed to be in the fcc structure for which the (111), (100), and (110) surfaces were considered. We have chosen to approximate the hcp structure of Y, Zr, Tc, and Ru by the fcc struc-

ture in order to facilitate a comparison across the series for the same surfaces; computationally, there is no advantage in this choice. For comparable fcc and hcp surfaces, we expect similar behavior. For Nb and Mo, results for the bcc (110) and (100) surfaces are presented as well. For each metal surface the results include the top-layer relaxation, the surface energy, and the surface-resolved work function. These quantities are discussed in view of the existing models. Furthermore, our all-electron method gives self-consistent core eigenvalues which can be compared to measured surface core-level shifts. This is planned to be presented in a future publication.

II. METHOD

The calculations presented here were done using the full-potential linear-muffin-tin-orbital (FP-LMTO) method as described in Refs. 11 and 12, with some modifications needed for an accurate description of surfaces. These concern the representation of the wave function, charge density, and potential outside the crystal. As in the well-known LMTO-ASA (atomic-sphere approximation) method, the basis set consists of atom-centered Hankel envelope functions which are augmented inside atomic spheres by means of numerical solutions of the radial Schrödinger equation. However, to obtain a unique definition in all parts of space, and in distinction to the LMTO-ASA method, the spheres are here taken as nonoverlapping. In both the ASA and the FP approaches, the atomic spheres are needed to define the LMTO basis set. In the ASA method, they have the additional function of prescribing the way in which the potential and charge density are approximated by a simpler, more tractable form, namely spherically averaged inside each sphere. The important improvement of the FP method is to eliminate this shape approximation, which is severe for low-symmetry systems such as surfaces. This makes it necessary to represent the charge density and potential accurately in the (now nonvanishing) interstitial region and to evaluate three-center integrals for the interstitial potential matrix elements. This is done in an efficient way by approximating the relevant quantities in the interstitial region as a linear combination of atom-centered Hankel functions which reproduces the values and slopes on the spheres. A further important (albeit straightforward) improvement over the LMTO-ASA method is that the nonspherical terms in the charge density and potential are retained inside the atomic spheres. In total, the effective potential, the electron density, the single-particle wave function, and the total energy are evaluated without significant approximation. One possible difficulty should be mentioned, however. The technique gives accurate results as long as the spheres are well packed in all those parts of space where the charge density is non-negligible. For slab calculations, it is therefore necessary to cover the surfaces with one or two layers of empty spheres; we have found that it is adequate to include all those spheres which are nearest neighbors of a metal atom. To obtain an accurate representation of the exponentially decaying density outside the surface, the empty-sphere angular-momentum cutoff for the explicit part of the sphere density and for the augmentation of the wave function was increased from the usual value of 4 to 6. The empty spheres are mainly a device for performing integrals over the interstitial region; they are not needed to increase the size of the basis set. Therefore, the basis consisted of LMTO's centered on the metal atom sites only. Due to the nonvanishing interstitial region it is not enough to use the minimal basis of the LMTO-ASA approach. A relatively large basis of 27 functions per metal atom was used, consisting of s, p, and d functions with kinetic energies of $-\kappa^2=-0.7$, -1.0, and -2.3 Ry; thus, the Hankel envelopes are exponentially localized as $e^{-\kappa r}$. The classical choice of the LMTO-ASA method, $-\kappa^2=0$, is not suitable for the surface since the wave functions decay exponentially into the vacuum with κ at least the square root of the work function.

The method was applied to seven-layer slabs, separated by approximately ten layers of vacuum. One layer of empty spheres was used for all the surfaces except the more corrugated (110) surface which required two empty layers. The **k**-space integration was done with special point meshes of 19, 15, 16, 20, and 15 irreducible points in one plane, for the fcc (111), (100), (110), and bcc (110) and (100) surfaces, respectively, with a Gaussian broadening of 20 mRy. Sphere radii were chosen to be 3% smaller than touching in the unrelaxed structure in most cases; the exception is the fcc (110) surface, which shows stronger relaxations and makes spheres 5% smaller than touching necessary.

The calculated surface relaxations depend very sensitively on the underlying lattice constant used for the slab. A good estimate of this effect can be obtained by assuming that the volume per atom will tend to be constant. The lattice constant was determined by careful bulk calculations, done with the same sphere radius and LMTO basis and a comparable **k** mesh as in the slab. Hereby the sphere radius was kept fixed as the volume was changed. Using a different sphere radius or scaling the radius along with the lattice constant leads to very small differences in the equilibrium geometry, which nevertheless can influence the relaxation noticeably. We have found it necessary to include the $4p$ semicore electrons as full band states through most of the series; this was done by means of a "two-panel" calculation for the metals from Y through Pd. All core states, including the low-lying ones, were permitted to relax ("thawed core"). Our calculation therefore distinguishes three types of states. Valence states are the $5s5p4d$ electrons, calculated with the FP-LMTO technique as described above. Semicore states are the $4p$ elections. In the two-panel technique, these are obtained by a second band-structure calculation, done with a basis of $5s$, $4p$, and $4d$ orbitals. All lower states (down to the $1s$ electrons) are recalculated in each iteration in the spheridized potential. The calculations were done nonrelativistically and the Ceperly-Alder parametrization[13] of the exchange-correlation potential was used. Only the top-layer relaxation was considered since it is in general weakly dependent on relaxation of the lower layers for transition metals (see below). All

metals were first assumed to have the fcc structure, in order to facilitate the study of trends and to avoid mixing in structural effects. While the fcc structure is a reasonable approximation for the hcp metals near the beginning of the series, it is artificial for the bcc metals Nb and Mo, for which it leads to unusual relaxation behavior. Therefore calculations were also done for the Nb and Mo bcc (110) and (100) surfaces.

To test our scheme, we compared our relaxation results to those of previous full-potential linear augmented plane wave (FLAPW) calculations where available. Feibelman and Hamann[7] have calculated the relaxation of the top two layers of a seven-layer Rb(100) slab, obtaining a contraction of the outer-layer separation d_{12} by 5.1% and of the second-to-third layer separation d_{23} by 0.5%. Our method gives contractions of 3.4% and 1.3% for this surface. Since Feibelman and Hamann used a scalar-relativistic procedure, we have calculated the top-layer relaxation of this surface both nonrelativistically and scalar relativistically, letting only the top layer relax, giving contractions of 3.5% and 3.7%, respectively. We conclude that scalar-relativistic effects influence the relaxation only slightly in the 4*d* series, even though the Rh bulk lattice constant reduces from 7.20 to 7.12 a.u. by the scalar-relativistic treatment. More significant is that our Rh(100) surface contraction increases by about 1% if the 4*p* states are approximated by treating them as core states; however, this result could be different for other methods, depending on how they handle high-lying core states which are not treated as band states. The most sensitive feature of our technique is the interpolation procedure for the interstitial region. The accuracy can be monitored by inspecting the change of the relaxation as the localizations of the Hankel functions in the charge-density basis are varied. The top-layer relaxation changed by no more than 0.2% as the first Hankel energy was varied from -0.5 to -4 Ry with the second energy fixed at -3 Ry. We conclude that the interpolation scheme is accurate for the systems considered here.

We have also calculated two-layer relaxations for the bcc W(100) surface (using the scalar-relativistic treatment in this case) in order to compare to the results of Fu *et al.*[8] Our relaxations of -8.3% and $+1.8\%$ for d_{12} and d_{23} agree reasonably well with their values of -5.8% and $+2.4\%$; both sets of results are well within the scatter of different experimental values[14] (ranging from $-7\pm1.5\%$ to $-8\pm1.5\%$). We speculate that the discrepancy in the two sets of calculated results could be due to the treatment of the quite extended W 5*p* states as true core states in the FLAPW calculations, whereas we treat them with the same accuracy as the valence states.

The results for the Rh(100) surface shows that the top-layer relaxation changes by only a small amount when the second layer is permitted to relax. For the two-layer relaxations of the Pd(100) surface, we obtain contractions of 0.4% for d_{12} and of 0.3% for d_{23}, to be compared to a contraction of 0.6% for d_{12} when only the top layer is permitted to move. This independence of the top-layer relaxation from the positions of the lower layers for transition metals (but not for *sp* metals[4]) was previously found for the W(100) surface.[8] Therefore, our trend study across the 4*d* series was restricted to top-layer relaxations.

Ho and Bohnen[4] have calculated the multilayer relaxations for the Ag surfaces using norm-conserving pseudopotentials and a mixed-basis scheme. The change in the top-layer spacing was -0.4%, -1.3%, and -7.4% for the (111), (100), and (110) surfaces. Because of the full Ag *d* shell, we expect the "softer" behavior typical for *sp* metals and a larger dependence of the top-layer relaxation on the shifts of the lower layers. Therefore, the agreement to our results (-1.4%, and -1.9%, and -3.6%), which kept all lower layers fixed, is acceptable. The fcc (110) surface is a special case because atoms in the top and third layers are nearest neighbors. An inward relaxation of the top layer moves these atoms directly toward each other. The pseudopotential calculation obtained an increase of the second-to-third layer spacing by 2% so that the disagreement in the top-layer relaxation is probably the consequence of keeping the lower layers fixed in our calculations.

III. RESULTS

The equilibrium Wigner-Seitz radii and bulk moduli for the nine metals are compared to the measured values[15] and the Korringa-Kohn-Rostoker (KKR) results of Moruzzi, Janak and Williams[16] in Fig. 1. As explained above, in the bulk calculations the spheres were kept at a fixed size in order to treat the bulk in the same way as the slab. The figure shows that there are only small changes when the sphere size is reduced from -3% to -5% of the touching muffin-tin radius.

Turning to the results for the surfaces of the Y to Ag series, we first compare the calculated and measured work functions in Fig. 2. Evidently there is good agreement of our surface-resolved values to the measured polycrystalline work functions.[17] Furthermore, the results for Ag show that the calculation predicts the correct surface dependence: the measured values are 4.74, 4.64, and 4.52 eV for the (111), (100), and (110) surfaces[18] compared to our calculated values of 4.67, 4.43, and 4.23 eV. The top-layer relaxation changes the work function by less than 0.1 eV even for those surfaces which exhibit a strong relaxation. For Nb and Mo, we find that fcc and bcc surfaces with comparable smoothness have similar values for the work function. The basis rising trend across the series follows closely that of the first ionization potential of the free atoms and is due to the highest occupied 4*d* level moving to lower energies with increasing nuclear charge. From Pd to Ag, part of the extra electron goes into the *sp* band above the full *d* band, increasing the Fermi energy and reducing the work function.

A. Surface energies

The surface energy σ of a solid is one half of the energy which is needed to cleave the crystal along some chosen plane. Thus, it is the energy associated with the creation of one surface. It depends on the choice of the plane and can be expressed either as an energy per surface atom or

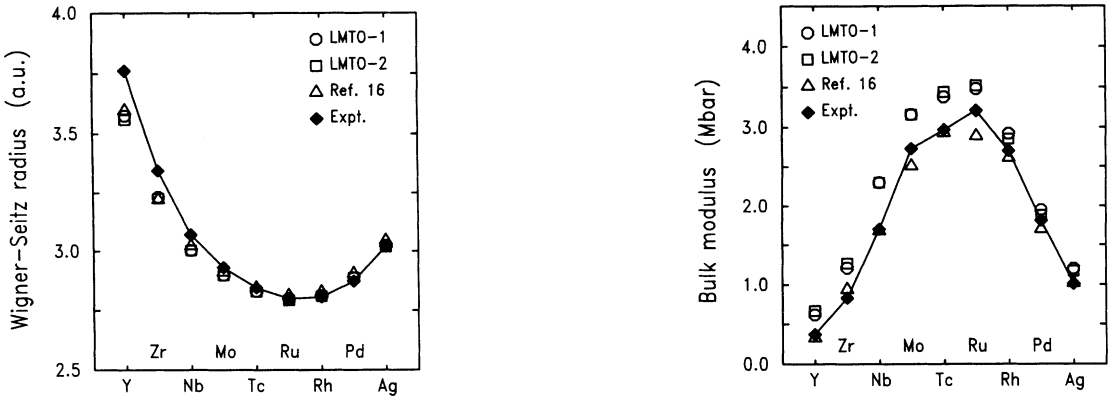

FIG. 1. Calculated equilibrium Wigner-Seitz radii (left) and bulk moduli (right) when atomic spheres with fixed radius 3% and 5% smaller than touching at the equilibrium lattice constant (LMTO-1 and LMTO-2, respectively) are used, as well as the results of Moruzzi, Janak, and Williams (Ref. 16) and the experimental values (Ref. 15).

per unit surface area. The calculation gives σ per surface atom as

$$\sigma=(E_{\text{slab}}-7E_{\text{bulk}})/2\ , \tag{1}$$

where E_{slab} and E_{bulk} are the total energies per unit cell of the seven-layer slab and the bulk crystal, respectively. The results for the series Y to Ag are tabulated in Table I and displayed in Fig. 3(a). Two features which are immediately evident are, first, that the surface energy shows the typical parabolic dependence on the d occupation which is already well known from the cohesive energy,[16,19] and, second, that the surface energy per surface atom increases with the roughness of the surface. In this section, we interpret the results within simple bond-cutting models as well as within more sophisticated models which take the dependence of the bond strength on the coordination number into account. It will be seen that the latter description is needed to reproduce relations between the surface energy and the cohesive energy which are known from experiment. Furthermore, we dis-

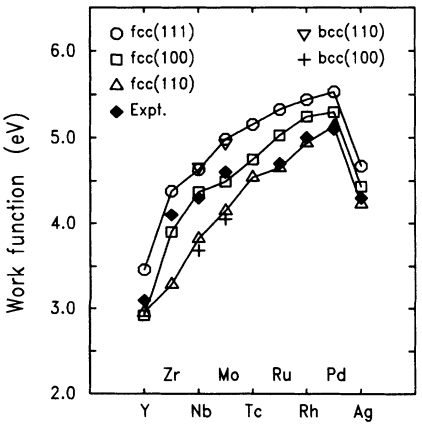

FIG. 2. Calculated surface-resolved work functions in eV as compared to the experimental polycrystalline values (Ref. 17).

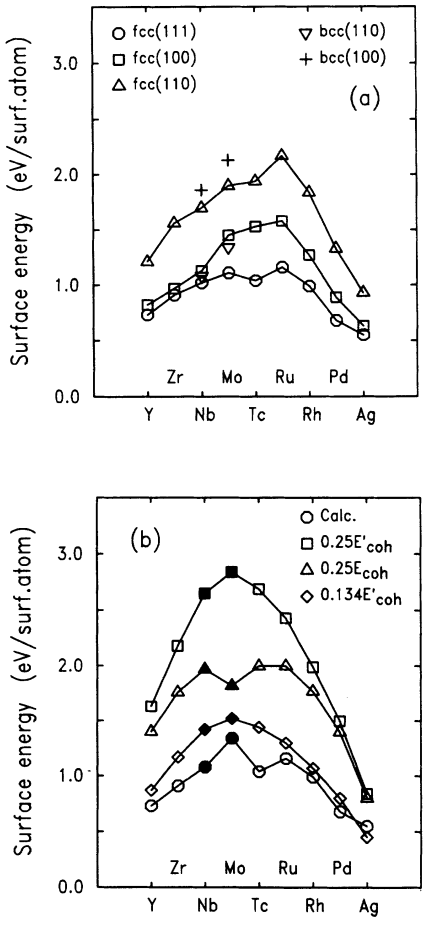

FIG. 3. (a) Calculated surface energies in eV per surface atom. (b) Comparison of the calculated surface energies with various multiples of the cohesive energy relative to the nonmagnetic (E'_{coh}) or magnetic (E_{coh}) free atom. Values are for the fcc (111) surface except for Nb and Mo, for which the bcc (110) surface was used (full symbols). The structure near Tc in the calculated surface energies is due to the change from bcc to fcc.

cuss the role of the free-atom orbital structure which was hitherto ignored.

The main features of the surface energy trends can be explained in a simple bond-cutting model. The strength of the nearest-neighbor d bonding is assumed to depend parabolically on the number of d electrons. It is maximal for a half-full band and small for an empty or completely full d band. The surface energy is then estimated as the energy cost for cutting the bonds to one nearest-neighbor atom times the number of removed nearest-neighbor atoms when the surface is created. In Fig. 3(a) one can see that the surface energies for the three fcc surfaces of each metal are roughly proportional to the number of removed nearest neighbors, which are 3, 4, and 6 for the fcc (111), (100), and (110) surfaces, respectively. For the bcc structure, the situation is more complicated because the eight nearest-neighbor (NN) distances are not much shorter than the six next-nearest-neighbor (NNN) distances. The bcc (110) surface cuts two NN and two NNN bonds, while the rougher bcc (100) surface cuts four NN and one NNN bond (in this discussion, we use "bond" to denote the total bonding strength due to occupied d orbitals between two atoms). If only the NN bonds are considered, the ratio of the (100) and (110) surface energies should be 2.0, whereas the calculation gives 1.7 and 1.5 for Nb and Mo, respectively. These numbers are less than 2.0 because the rougher (100) surface cuts a smaller number of NNN bonds. All together, this simple description seems to give a quite consistent picture which can explain the basic parabolic trend and the surface dependence of the surface energy.

In the past, the bond-cutting model has often been invoked in order to deduce a relation between the surface energy and quantities such as the heat of sublimation.[20–23] These approaches try to explain the empirical evidence[22] that for many liquid metals σ is approximately one sixth of the heat of vaporization.[24,25,20] Similarily, for solid metals σ is often close to one sixth of the heat of sublimation; below we will reconsider this relation. Assuming that the energy for cutting a single bond is a well-defined quantity, then there should be a simple relation between the surface energy (the energy cost when some bonds are cut) and the heat of sublimation (the cost when all bonds are cut). The heat of sublimation is equal to the cohesive energy within the accuracy of this description and we use the terms interchangeably in the

TABLE I. Summary of calculated results: top-layer relaxation in percent of the unrelaxed layer spacing, work function, surface energy per surface atom, and surface energy per unit surface area. Surface energies are for the relaxed surfaces.

	Surface		Δd_{12} ($\%d_{12}$)	Work function (eV)	Surface energy (eV/atom)	Surface energy (J/m^2)
Y	fcc	(111)	−3.3	3.46	0.73	1.15
	fcc	(100)	−4.7	2.92	0.82	1.12
	fcc	(110)	−2.0	2.95	1.21	1.18
Zr	fcc	(111)	−2.5	4.38	0.91	1.75
	fcc	(100)	−4.2	3.90	0.97	1.62
	fcc	(110)	−5.5	3.29	1.56	1.85
Nb	fcc	(111)	0.3	4.63	1.02	2.20
	fcc	(100)	−0.6	4.37	1.13	2.11
	fcc	(110)	−9.4	3.82	1.70	2.26
	bcc	(110)	−3.7	4.66	1.08	2.36
	bcc	(100)	−9.3	3.68	1.86	2.86
Mo	fcc	(111)	−0.8	4.98	1.11	2.64
	fcc	(100)	−1.9	4.49	1.45	2.98
	fcc	(110)	−14.2	4.15	1.90	2.77
	bcc	(110)	−3.9	4.94	1.34	3.14
	bcc	(100)	−9.0	4.05	2.13	3.52
Tc	fcc	(111)	−4.9	5.15	1.04	2.63
	fcc	(100)	−5.1	4.75	1.53	3.34
	fcc	(110)	−13.0	4.54	1.94	3.00
Ru	fcc	(111)	−3.9	5.33	1.16	2.99
	fcc	(100)	−4.4	5.03	1.58	3.52
	fcc	(110)	−9.7	4.65	2.17	3.45
Rh	fcc	(111)	−2.5	5.44	0.99	2.53
	fcc	(100)	−3.5	5.25	1.27	2.81
	fcc	(110)	−7.5	4.94	1.84	2.88
Pd	fcc	(111)	−0.1	5.53	0.68	1.64
	fcc	(100)	−0.6	5.30	0.89	1.86
	fcc	(110)	−5.3	5.13	1.33	1.97
Ag	fcc	(111)	−1.4	4.67	0.55	1.21
	fcc	(100)	−1.9	4.43	0.63	1.21
	fcc	(110)	−3.6	4.23	0.93	1.26

following. If C_B is the coordination number in the bulk and ε is the energy of a single nearest-neighbor bond, then the cohesive energy per bulk atom is $E_{\rm coh}=\frac{1}{2}C_B\varepsilon$. A surface atom has a lower coordination number C_S so that C_B-C_S bonds must be cut to make the two new surfaces. The desired proportionality is then given[26] by

$$\sigma=\frac{C_B-C_S}{C_B}E_{\rm coh}\ . \tag{2}$$

The energy cost of cutting a nearest-neighbor bond is an acceptable concept for strongly covalent materials such as diamond, but it is not obvious that a similar approach (also known as "quasichemical theory"[21]) will work for metals. Our calculation supplies both σ and $E_{\rm coh}$, so that the assumptions leading to Eq. (2) can be tested directly.

Before this can be done, the role of the energy gain due to the magnetic ordering in the free atom should be clarified. This spin-polarization energy is in the range of 0.1–0.2 eV for *sp* metals, but is larger for transition metals near the center of the series (i.e., 4 eV for Mo) and becomes comparable to the cohesive energy. We denote by the spin-polarization energy the difference of the free-atom total energies calculated using the local-spin-density approximation (LSDA) and the local-density approximation (LDA). A correlation between different energies according to the bond-cutting model can only be expected if systems of the same type are compared. When the nonmagnetic crystal is "vaporized" by cutting bonds, from a theoretical viewpoint we can consider that first a nonmagnetic free atom results, and it is the energy cost of this step (here denoted $E'_{\rm coh}$) which can be expected to correlate with the surface energy. In a second, conceptually unrelated step the free atom relaxes to its magnetic ground state according to Hund's rules. The experimental cohesive energy is the sum of both terms, so there seems to be a basic flaw in the simple "quasichemical approach" [see Eq. (2)] to surface energies, which should be of particular importance when applied to elements near the middle of the transition-metal series.

Figure 3(b) presents the calculated data in a way which should make visible a correlation between the surface and cohesive energies. The smoothest surface for each structure, i.e., fcc (111) and bcc (100), were taken for this example. For both surfaces the simple bond-cutting model predicts that σ is equal to $E'_{\rm coh}/4$ [this is Eq. (2) with $E_{\rm coh}$ replaced by $E'_{\rm coh}$]. This estimate of the surface energy turns out to be considerably too large. If one insists despite better knowledge on using the full (spin-polarized) cohesive energy, the result is not much better. One sees that $E_{\rm coh}/4$ is also too large, and in fact gives a less satisfactory representation due to the atomic spin-polarization-induced dip at Mo. This was anticipated in the discussion of the free-atom energy above. The reason for the failure of the simple quasichemical model is that the variation of the bond strength with the coordination number C was not taken into account. It is well known that the bonds are stronger for an atom with a smaller number of neighbors. Making a fcc (111) surface entails cutting the twelfth, eleventh, and tenth bonds, which are comparatively weak, whereas all 12 bonds must be cut to "vaporize" the crystal. Consequently, the straightforward bond-cutting model overestimates the surface energy. The coordination-number–bond-strength relation has recently been calculated explicitly for Al by means of total-energy calculations for a variety of structures with C between 0 and 12 by Robertson, Payne, and Heine.[27] The energy per bond is found to be more than twice as large for $C=2$ than for $C=12$. The effect can be quantified using results of tight-binding theory. In the second-moment approximation, the width of the local density of states on an atom scales with C, leading to an energy gain proportional to $C^{1/2}$ due to the lowering of the occupied states. Neglecting repulsive terms for now, the energy per nearest neighbor is then proportional to $C^{1/2}$. By assuming that the crystal total energy is the sum of contributions from the atoms, each of which is proportional to the square root of its coordination number, it follows that the surface energy is given by

$$\sigma=\frac{C_B^{1/2}-C_S^{1/2}}{C_B^{1/2}}E'_{\rm coh}\ . \tag{3}$$

For the fcc (111) and bcc (110) surfaces, the proportionality factor is now 0.134 and thus about half of the previous value. Figure 3(b) shows that this relation between the surface and cohesive energies is in reasonable agreement with the calculated results. Of course, this is a rather oversimplified version of the tight-binding formalism, which is not complete because repulsive forces are not taken into account. The repulsive energy contributions lead to an additional linear term in the total energy as function of C.[27] Using such an expression, with the linear coefficient fixed at the typical value 0.1 eV, the estimated surface energies decrease by 10–20 % which improves the agreement some more.

Combining the effects of the bond-strength–coordination-number relation and the free-atom spin polarization, the empirical result of 0.16 for $\sigma/E_{\rm coh}$ (both expressed as an energy per mole) for solids can be explained. To begin with, the calculated results (Table I) show that the surface energy per surface atom depends strongly on the choice of the surface; it is the surface energy per unit area which is relatively invariant. The connection between the two quantities is given by the molar surface area, which varies with the roughness of the surface. The surface energy for polycrystalline solids is customarily assumed to be close to that of the most dense surface[23] since this minimizes the surface energy per unit area. Similarily, it is assumed that the molar surface area for liquid metals is related to the third root of the liquid density by a similar factor. Therefore we again consider the fcc (111) and bcc (110) surfaces. For these, the surface energy can be estimated by $0.134E'_{\rm coh}$ [see Fig. 3(b)]. For *sp* metals and near the ends of each transition metal series, the energy gain from the magnetic moment of the free atom is small but in general not negligible, giving values of $E_{\rm coh}/E'_{\rm coh}$ which vary between 1.0 (when the atom is nonmagnetic) and about 1.20. The product of 0.134 with this factor then gives an estimate of $\sigma/E_{\rm coh}$ which varies from 0.134 to 0.16. For metals near the middle of the transition series, the ratio of surface to

cohesive energy should be larger. It is interesting to see whether this can be found in the experimental data. We have therefore plotted the ratios of the surface energy to the heat of vaporization for the liquid elemental metals where the data is available (Fig. 4). We are conscious that this presentation tends to emphasize the deviations from the rule as opposed to plotting one quantity against the other. Unexpectedly, the ratios for the elements at the center of the transition series (e.g., Mo) are not noticeably higher. This is in disagreement with our calculated results, for which the self-consistently calculated ratio $\sigma/E_{\rm coh}$ of Mo is significantly above that of the other metals. Overall the agreement to the experimental values is good for the surface energy (see below) as well as for the cohesive energy, so the discrepancy to the $\sigma^{\rm expt}/E_{\rm coh}^{\rm expt}$ ratio is puzzling. Closer inspection traces the discrepancy to the cohesive energy: while most of the metals are overbound by about 15–20 % in the calculation, for Mo the cohesive energy lies only 5% above the experimental value. In fact, if the von Barth–Hedin exchange-correlation potential is used, no overbinding at all is found for Mo.[29] This unusual dependence on the choice of the LDA potential is due to the different spin-polarization energies for the $5s^1 4d^5$ Mo free atom, which are 4.07 and 4.44 eV for the Ceperly-Alder and von Barth–Hedin potentials, respectively. These features point to the inadequate treatment of the free atom in the LDA as the source of the discrepancy in $\sigma/E_{\rm coh}$. It is intriguing that a better treatment than the LDA would presumably put Mo back into line with the other metals, despite the large magnetic moment and our previous arguments; should this not be an accident, it would pinpoint an error of the local density approximation.

An unexpected feature of the $\sigma^{\rm expt}/E_{\rm coh}^{\rm expt}$ values plotted in Fig. (4) is that ratios as large as 0.3 appear for some *sp* metals. These are consistently the group II (A and B) elements, which were not included in earlier studies.[22,30] Our explanation is that for these metals, the free atoms are especially stable due to the full *s* shell. This decreases the cohesive energy relative to the surface energy. The free-atom total energy is influenced by factors which do not play a role for the bulk and the surface, in this case the full shell of two *s* electrons which are redistributed between *s* and *p* states in the crystal. Expressed in a different way, it is the cohesive energy which shows unusual variation across the periodic table, while the surface energy is well behaved. In conclusion of this discussion, the popular approach to relate the surface energy with the cohesive energy erroneously includes the effect of the orbital structure on the free-atom total energy. This effect is largely quenched out in the solid bulk as well as at the surface, making the straightforward approach highly problematic.

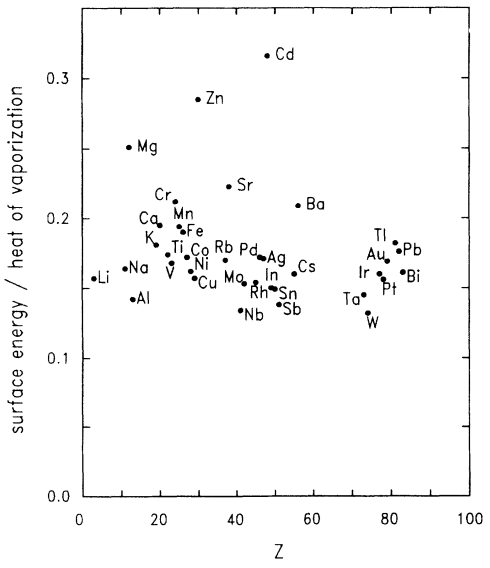

FIG. 4. Ratio of the surface energy to the heat of vaporization $\sigma^{\rm exp}/\Delta H_{\rm vap}^{\rm expt}$ for a number of liquid metals where available experimental data exists (Ref. 28).

Returning briefly to the simple bond-cutting picture, in view of the preceding discussion it would seem a contradiction that the dependence of the surface energy on the surface plane could be reproduced without including the variation of the bond strength with the coordination number. The answer is that, in order to obtain the surface energy proportional to the number of cut bonds, it is sufficient to assume that the energy of an atom depends on its coordination as $E = C\varepsilon + E_0$ where E_0 is some constant. The linear relation is a good approximation when C is larger than about 5. This defines an effective bond strength suitable for comparing highly coordinated structures. We emphasize, however, that this is much smaller than the bond strength which would be deduced from the cohesive energy by the simple bond-cutting model.

As stated above, the surface energy of solids is difficult to measure directly and few reliable results are available. On the other hand, the surface energy in the liquid state has been determined accurately for most elemental metals. Tyson and Miller[31] have used this data to estimate the solid metal surface energy for a closed-packed surface as function of the temperature. A related procedure was followed by Miedema.[32] Alternatively, Mezey, and Giber[23] have estimated the solid surface energies for most elemental metals from the heat of sublimation (denoted as enthalpy of atomization in their work) along the lines described above. Figure 5 compares these results to our surface-averaged calculated values. The agreement to the approaches of Tyson and Miller and Miedema is good. Some deviations are found near the center of the series. This is where we find the largest dependence on the surface orientation, which suggests that there are relevant structural effects which are outside the scope of the liquid metal estimate anyway. The agreement to the estimates from the atomization enthalpies (data marked by triangles in Fig. 5) is somewhat poorer. Figure 5 also shows that the uncorrected liquid metal surface energy is a rather poor estimate, although it is sometimes compared directly to theoretical results.[33]

Next, we compare to the results of previous calculations of the surface energy. Table II shows results obtained with the FLAPW method by various groups, which agree well with our values. For Pd, the FLAPW result of Ref. 34 is somewhat larger and in fact a bit

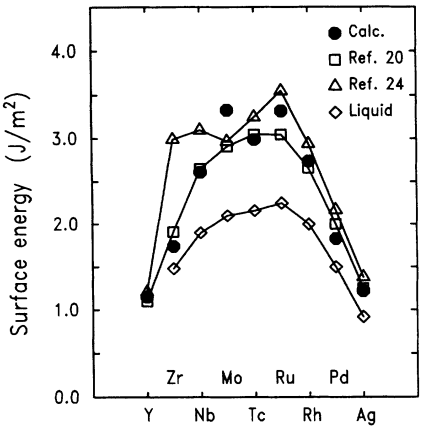

FIG. 5. Calculated surface energy (averaged with equal weights over the three fcc or two bcc surfaces) in J/m^2 compared to experimental estimates. The experimental values were deduced from liquid metal surface energies by Tyson and Miller (Ref. 31) and deduced from enthalpies of atomization by Mezey and Gilber (Ref. 23). For comparison the measured liquid metal surface energies (Ref. 28) are shown as well.

closer to the experimentally derived surface energy of Ref. 31. Also shown are the values obtained from simulations using semiempirical Finnis-Sinclair potentials[35] and the embedded-atom method.[36] These surface energies are too small by 30-50%. The Finnis-Sinclair potentials are based on tight-binding theory in the second-moment approximation, and the embedded-atom method is similar in practice although based on a different starting point. Comparing with results of tight-binding calculations in the moment representation,[37,33] the underestimated surface energies would seem to be a general property of the second-moment methods. Finally, Smith and Banerjea[38] have used a "universal bonding relation" to obtain surface energies for the three Ag surfaces. These show an unrealistically large surface dependence which none of the other calculations exhibit.

To mention another theoretical approach, we note that the ratios of the energies of different solid surfaces are predicted by the "liquid drop model"[39] to be $\sigma_{100}/\sigma_{111}=1.06$ and $\sigma_{100}/\sigma_{111}=1.20$ for the fcc structure and $\sigma_{100}/\sigma_{110}=1.14$ for bcc. The model expresses the total energy as a sum of volume, surface, and curvature terms. Our calculated energies lead to ratios which vary between 0.95 and 1.20 but which only partly group around the predicted values. Possibly, the more localized and directed d bonds result in more complicated behavior than that of nearly-free-electron metals.

To close this section, we refer to a paper by Krotschek and Kohn[40] which compares the local-density approximation to a variational theory based on minimization of the Fermi hypernetted-chain approximation for the ground-state energy. The aim is to study the validity of the local-density approximation for surfaces. From the application to jellium slabs, the authors conclude that the local-density approximation leads to unacceptable errors in the calculated surface energies for simple metals. They do not discuss the case of transition metals; however, it is noteworthy that our calculated surface energies are much closer to the experimental estimates than their results would lead us to expect. Specifically, we obtain good agreement for Ag, for which a treatment as a simple metal should be reasonably valid. In agreement with earlier publications (e.g., Ref. 41), we conclude that the neglect of atomic structure is the most severe approximation in a jellium-LDA approach when calculating surface energies. If the atomic structure is taken into account, the DFT-LDA theory gives quite accurate results.

B. Models for surface relaxations

Our aim is to compare the various models for metal surface relaxation with the results of our realistic LDA electronic-structure calculations. We briefly present three models. The best-known model is that of Finnis and Heine,[42] which is based on the concept of Smoluchowski smoothing.[43] Starting from the perfect crystal, an artificial surface is made by cutting along the boundaries of the Wigner-Seitz cells, without letting the charge density relax. The electrostatic force on each nucleus is then practically zero because of the symmetry

TABLE II. Comparison of present calculated surface energies in J/m^2 with results of full-potential LAPW calculations, semiempirical simulations, and the values of Smith and Banerjea.

			Present result	FLAPW Ref. 34	FLAPW Ref. 8	Semiempirical Ref. 35	Semiempirical Ref. 36	Smith and Banerjea Ref. 38
Nb	bcc	(110)	2.36	2.9		1.67		
	bcc	(100)	2.86	3.1		1.96		
Mo	bcc	(110)	3.14			1.83		
	bcc	(100)	3.52			2.10		
Rh	fcc	(100)	2.81		2.6			
Pd	fcc	(111)	1.64				1.22	
	fcc	(100)	1.86	2.3			1.37	
	fcc	(110)	1.97	2.5			1.49	
Ag	fcc	(111)	1.21			0.62	0.62	1.27
	fcc	(100)	1.21	1.3		0.76	0.71	1.63
	fcc	(110)	1.26	1.4		0.81	0.77	1.54

and neutrality of each Wigner-Seitz cell; the only nonvanishing force is due to high multipoles, i.e., $l \geq 4$ in structures with cubic symmetry. In a second step the electron density is permitted to relax to the correct ground-state distribution. Hereby the density becomes smoother (in order to reduce electron kinetic energy). The difference of the unrelaxed and relaxed densities causes an additional electrostatic potential (see Fig. 6) which modifies the surface dipole barrier and the work function, as was discussed in the original paper by Smoluchowski. Finnis and Heine later pointed out that the charge redistribution also gives rise to an inward electrostatic force on the top-layer nuclei. Obviously this smoothing effect is more pronounced for rougher surfaces. Thus, the Finnis-Heine model explains two basic observed phenomena: the inward relaxation and its dependence on the surface roughness. Quantitative predictions have been obtained by assuming a perfectly planar boundary for the electron density;[44] however, the resulting relaxations are considerably larger than the measured values. A modified point-ion model has been devised which includes an extra semiempirical term and can be adjusted to give better agreement to experiment.[45]

A second model focuses on transition metals and on the contribution of the *d* electrons to the surface relaxation. According to Pettifor,[46] the bulk lattice constant of a transition metal balances the inward force of localized *d* bonds against the homogeneous outward pressure of the *sp* electrons. As discussed in Refs. 47 and 8, at the surface the *sp* pressure can escape into the vacuum ("spill-out"), while the *d* bonds between the first two layers are essentially unchanged. These *d* electrons therefore exert an inward force on the surface atoms, leading to an additional relaxation contribution specific to transition metals. The additional inward force is proportional to the strength of the *d* bonds, and should therefore obey the classical bonding-antibonding parabola as a function of the *d* occupation. The largest inward force should be found for a half-full *d* band, since in this case all the bonding states and none of the antibonding states are filled. The parabolic behavior is well known from the cohesive energy and the lattice constant of the bulk transition metals (see Fig. 1). The situation is different for the noble metals because for these the *d* shell is full, leading to a repulsive force which now must be compensated by an attractive term from the *sp* electrons. Consequently it has been predicted that the top-layer relaxation should be outward for the noble metals.[47]

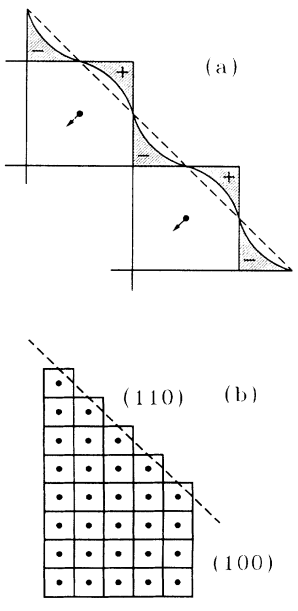

FIG. 6. Schematic illustrations of Smoluchowski smoothing (from Ref. 43). (a) shows the redistribution of the charge density at the surface when the density relaxes; (b) shows the dependence of the smoothing effect on the surface roughness.

In addition to these effects, yet another contribution comes from the bond strength—coordination number relation, first formulated by Pauling,[48] which was discussed above in the context of surface energies. This states that bonds are stronger on an atom with a smaller number of neighbors. For a surface, this means that the *d* bonds on the surface atoms should be stronger than those in the bulk.

Finally, tight-binding models have been used to investigate the way in which the wave function of the infinite crystal is modified when a surface is introduced. Analytic expressions have been obtained for the exact solution of the tight-binding Hamiltonian for a semi-infinite chain of *s* orbitals.[49] The force on the surface atoms, as deduced by comparing the top-layer and bulk-bond orders, leads to an outward relaxation for a nearly empty or a nearly full band, and an inward relaxation for a half-full band. The outward relaxation for the nearly empty band arises as a consequence of the less perfect bonding character near the surface for the "in-phase" bonding states near the bottom of the band. Occupation of such a state strengthens all the bonds in the crystal, but those in the bulk more than those at the surface. The outward relaxation for the almost-full band is understood in a complementary argument, as is usual for tight-binding models. In view of the experimentally deduced outward relaxation for Pd and Rh, this model could have a bearing on the realistic case.

We also mention that more approximate techniques based on the tight-binding method have been introduced. Allan and Lannoo have used the second-moment approximation to derive explicit expressions for the total energy of a semi-infinite crystal. The energy is the sum of a bonding term which describes the lowering of occupied states due to neighbor interactions, plus an empirical pairwise-repulsive term. The bonding term is obtained by fitting a Gaussian density of states to the zeroth, first, and second moments. A success of the approach is that it explains the existence of oscillatory multilayer relaxations in a simple way.[50] The dependence of the surface relaxation on the *d* occupation in transition metals has also been studied. In a first work, the relaxation was found to be inward in the center of the series, outward near the wings, and to change discontinuously to zero as the occupation increases toward ten or decreases toward zero.[51] Later it was recognized that this model is in fact unstable

for nearly full and nearly empty bands due to the inadequate treatment of charge transfer. By including local charge neutrality in a modified tight-binding scheme, the instability was removed.[52] The surface relaxation then turns out to be independent of the d occupation and always directed inward for the top layer, and to increase with increasing surface roughness. The same results are obtained in the non-self-consistent approach if a rectangular shape for the local density of states is used in place of the Gaussian shape.[37] These descriptions are rather incompatible with one of our main conclusions, namely that the competition between sp and d electrons leads to a basically parabolic shape of the relaxation trend (see below).

C. Surface relaxations

Our results for the top-layer relaxations are summarized in Table I and Fig. 7, which displays the change Δd_{12} of the first-to-second layer spacing d_{12} for the fcc (111), (100), and (110) surfaces, which have roughnesses 1.10, 1.27, and 1.80, respectively. (The roughness is defined in Ref. 53 as the reciprocal of the surface packing fraction when the crystal is packed with touching spheres). Also included are the relaxations for Nb and Mo bcc (110) and (100) surfaces with roughnesses 1.20 and 1.70, respectively. The figure shows that Nb and Mo in the fcc structure have anomalous relaxations close to zero for the two smoother surfaces. We consider this unusual behavior a consequence of the imposed artificial fcc structure. More precisely, Fig. 8 shows that the density of states (DOS) for the top-layer atoms in the Nb fcc (111) surface has a strong peak at the Fermi energy. It consists of L-derived states which also cause the peak in the bulk fcc DOS and which are partly the reason that fcc Nb and Mo are not stable respective to bcc. The lower part of the figure shows the change in the top-layer DOS when the outermost atoms are moved outward. One (expected) effect is that the d band becomes more narrow; the energy associated with this change is in line with the more general discussion below. A second effect is that the peak at the Fermi energy becomes wider and shifts somewhat to lower energies. It is reasonable to assume that this drives the anomalous outward relaxation. Consequently, the following discussion is restricted to the marked trends which connect fcc and bcc surfaces of similar roughness. The main features are as follows. (i) There is basically a parabolic character, showing stronger inward relaxation near the center of the series; this effect dominates for the fcc (110) surface. (ii) While no outward relaxations are found, Pd is a special case with Δd_{12} close to zero for the two smoother surfaces. (iii) From Pd to Ag for the fcc (111) and (100) surfaces, the trend reverses as Ag again shows a substantial inward relaxation. This is contrary to the prediction of Ref. 47, which predicts an outward relaxation for noble metals due to the repulsive force of the full d shell. Below, we associate the reversal of the trend with the increase of sp electrons from Pd to Ag.

The most obvious feature is the parabolic character, which is well known from the bulk lattice constant and cohesive energy. As the d occupation increases across the series, the strength of the localized bonds first increases (as bonding d states are filled) and then decreases (as the antibonding d states are filled). The localized d bonds give rise to a force which tends to contract the bulk material, compensated by the outward pressure of the sp electrons. As suggested in Ref. 8, at the surface the sp pressure spills out into the vacuum, resulting in a net inward force from the d bonds. Given the dependence of the d-bond strength on the occupation, this model can explain the basic parabolic shape of the calculated relaxations. This reveals why the second-moment tight-binding approach[52,37] obtains a relaxation which is independent of the d occupation, in disagreement with the present *ab initio* results. Since the most important ingredient is the strength of the d bond relative to the sp pressure, the parabolic shape cannot be obtained if the sp electrons are not included in some way.

It is not yet clear why the whole parabola is deeper for the rougher (110) surface. The shape of the curve suggests an explanation based on the d electrons here also, as

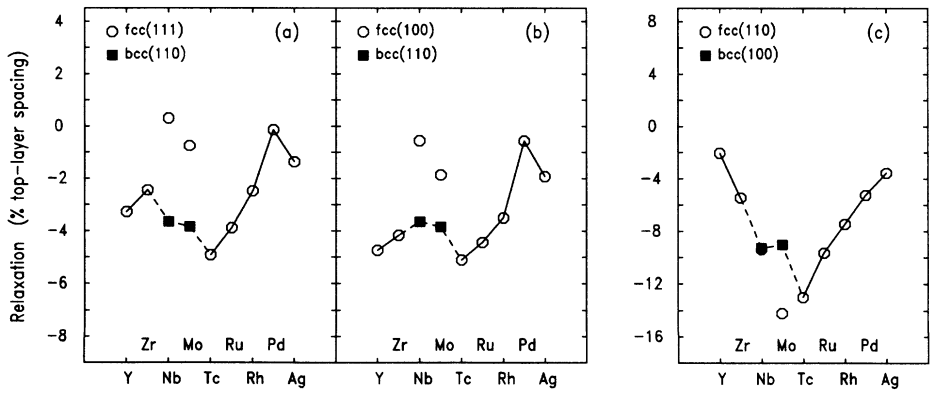

FIG. 7. Calculated top-layer relaxations for the series Y through Ag in percent of the bulk interlayer spacing. Relaxations for the fcc structure are shown as circles, for the bcc structure as squares. The lines connect fcc and bcc surfaces with similar roughnesses: (a) fcc (111) and bcc (110) with roughness 1.10 and 1.20; (b) fcc(100) and bcc(110), roughness 1.27 and 1.20; (c) fcc (110) and bcc (100), roughness 1.80 and 1.70.

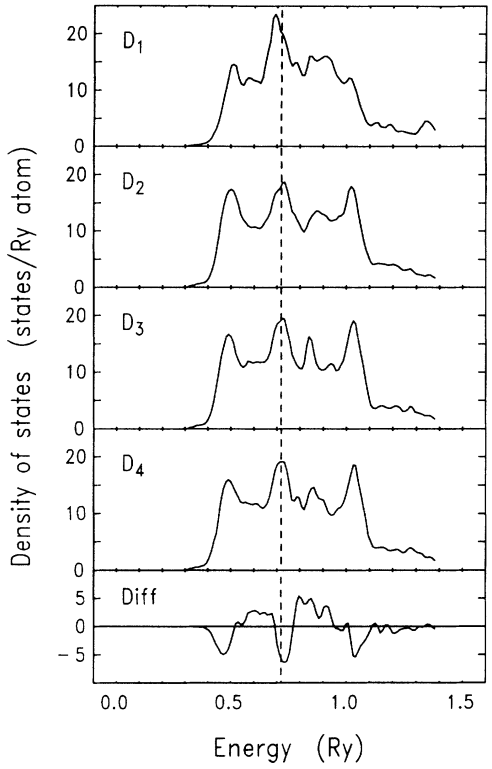

FIG. 8. Layer-resolved density of states for the Nb fcc (111) surface. D_1 is for the outermost layer, D_4 is for the center layer of the slab. The bottom panel shows the change in D_1 when the top layer moves from a position relaxed inward by 6% of the layer spacing to a position relaxed outward by 6%.

opposed to the smoothing argument normally associated with the *sp* electrons. First, each cut *d* bond at the surface eliminates a nearest-neighbor attractive force which has an outward component on the top-layer atom. The resulting inward force on the surface atom is larger for a rough surface since more bonds are cut. Second, cutting some of the bonds on an atom enhances the strength of the remaining ones. This again leads to a larger inward force for a rougher surface. The combination of these effects governs the relaxation of the (110) surface. In this explanation, the smoothing effect due to the *sp* electrons is also present but the total relaxation is dominated by the *d* electrons.

For the (111) and (100) fcc surfaces, which are smoother, the effect of the *d* electrons is not as strong and an interplay of different effects is seen. Specifically, the inward relaxation due to *sp*-electron smoothing is not swamped out. To model this, we consider a description which combines the characteristic effects of the *sp* and *d* electrons.

$$\Delta d_{12} = -AQ_{sp} - B[1-(1-Q_d/5)^2] , \tag{3}$$

where Q_{sp} and Q_d are the *sp*- and *d*-electron charges per atom and $A,B>0$ are constants. The first term describes the inward relaxation due to Smoluchowski smoothing, which for simplicity is assumed to be proportional to the *sp* charge. The second term is an inward relaxation which depends parabolically on the amount of *d* charge. To obtain the decomposition of the total valence charge into angular momentum contributions [Fig. 9(a)], the localization of the LMTO basis functions was exploited to make a Mulliken population analysis[54] for the bulk. These charges were substituted into the model expression with $A=3$ and $B=2$ to obtain the curve in Fig. 9(b). The main features of the calculated relaxations are reproduced. The basic parabolic behavior is thus due to the variation of the *d*-bond strength with *d* occupation. The parabola is not symmetric because Y already has more than two *d* electrons. The kink in the trend at Pd, i.e., the inward relaxation of Ag compared to Pd, comes about because Pd already has an almost-full *d* band ($Q_d=9.4$). Thus the extra electron when going from Pd to Ag can only partly go into the *d* band; however, at the antibonding end, each extra *d* electron decreases the inward relaxation from the localized *d* bonds. On the other hand, the large increase of the *sp* charge increases the inward relaxation effect of the Smoluchowski smoothing. These two factors work together for the step Pd to Ag, whereas the *sp* and *d* terms tend to cancel for the rest of the series.

We believe that the main effects are contained in the above description which combines the effect of *sp*

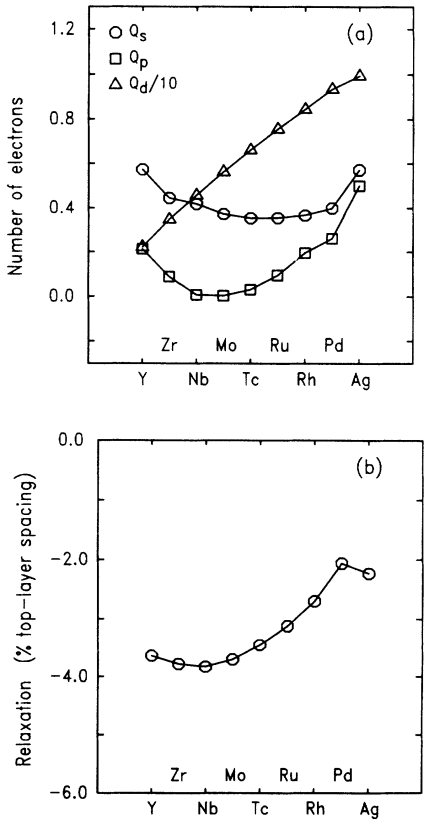

FIG. 9. Model relaxation for the smoother surfaces based on *sp* electron smoothing and localized *d* bonds; (a) decomposition of the bulk charge into *s*,*p*,*d* contributions; (b) result of the *sp* + *d* model using the charges of (a).

smoothing with localized *d* bonding. However, comparing Fig. 9(b) with the calculated relaxations, one sees that there is one feature which the model does not describe correctly. The calculated result for the Pd(111) and (100) surfaces is a top-layer relaxation close to zero, while the model must give an inward relaxation of some percent if the shape of the curve is to be reasonably reproduced. The discrepancy is not unexpected, since the effect of both the *sp* and the *d* electrons has been taken to be an inward relaxation. This suggests that some effect is still omitted. Furthermore, the calculated curves show a deeper parabola than the model. The parabola of the model can be made deeper by increasing the parameter B, but this then makes the relaxations for Pd and Ag almost equal. This discrepancy could be a consequence of oversimplification (for example, from assuming a linear dependence on the *sp* charge) but could also point to an omitted effect. In a more speculative manner, one can remedy the discrepancies by invoking the results from the semi-infinite chain of tight-binding *s* orbitals. Formally, this is not unreasonable because the terminated *d* metal is equivalent to an ensemble of semi-infinite chains, each of which has *s*-type symmetry along the sequence of layers. Qualitatively this would lead to an extra energy term which causes larger inward relaxations in the middle of the series, and a larger outward relaxation in Pd due to the nearly full *d* band.

To see if some features of this tight-binding description can be explicitly recovered from the calculated results, we divided the energy interval of the Pd *d* band into three ranges, corresponding roughly to bonding, nonbonding, and antibonding states (Fig. 10). Figure 11 shows the charge density of the Pd(100) surface for the three ranges and the total density. To make a comparison between the densities easier, each one was normalized to make the charge on a bulk Pd atom equal to one. As a measure for the bond strength, we consider the value of the charge density in the center of a nearest-neighbor bond. The density for the lowest energy range shows the expected feature, namely that states at the bottom of the band show stronger bonding inside the crystal than between the top two layers. In the tight-binding description, a state near the top of the band weakens all bonds, but those inside the crystal by a larger amount. Therefore, deoccupying such a state (from the inert completely full case) strengthens the bulk bonds relative to those at the surface and causes an outward surface relaxation. In short, a state near the top of the band should be more bonding near the surface than deep inside. There is only a very small indication of this in the density of the third energy range in Fig. 11. Of course, in a self-consistent calculation the situation is obscured by the response of the potential to charge redistribution, so that a direct correspondence to the tight-binding model is not necessarily to be expected. One consequence of self-consistency is that the more narrow local DOS of the top layer shifts upward in energy in order to maintain its position relative to the bulk Fermi level in order to achieve local charge neutrality. This is visible in Fig. 10 and is a well-known explanation for the core-level shifts in transition metals.[55] Associated with this energy shift will be some rearrangement of charge whose significance is not obvious; conceivably, it could also have a direct consequence for the surface relaxation.

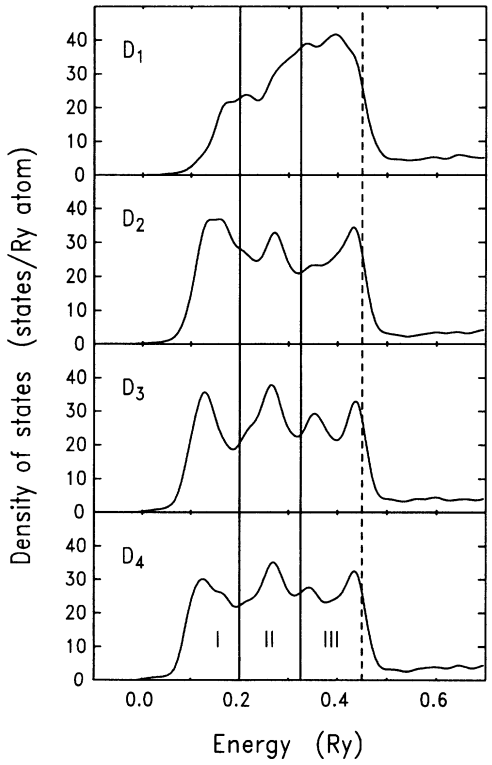

FIG. 10. Layer-resolved density of states for the Pd(100) slab. D_1 is for the top layer, D_4 is for the center layer of the seven-layer slab. The energy range is roughly divided into bonding, nonbonding, and antibonding states.

IV. CONCLUSIONS

In conclusion, we have calculated surface energies, the work functions, and the top-layer relaxation of the fcc (111), (100), and (110) surfaces for the 4*d* transition metals Y to Ag and for the bcc (110) and (100) of Nb and Mo. Good agreement to the measured work functions is found, for the average trend across the series as well as for the surface dependence. However, for most of the studied materials the surface dependence is a theoretical prediction. The surface energy shows the parabolic dependence of the *d*-band occupation, which is known from the cohesive energy and is roughly proportional to the number of nearest neighbors which are removed when the surface is created. The results were discussed in the context of popular models which relate the surface energy to quantities such as the cohesive energy or the heat of sublimation. It was shown that these models only work if the change of the bond strength with the coordination number is taken into account. Furthermore, it was found that the popular approach erroneously includes energy contributions due to the free-atom orbital structure in the estimate for the surface energy, as can be

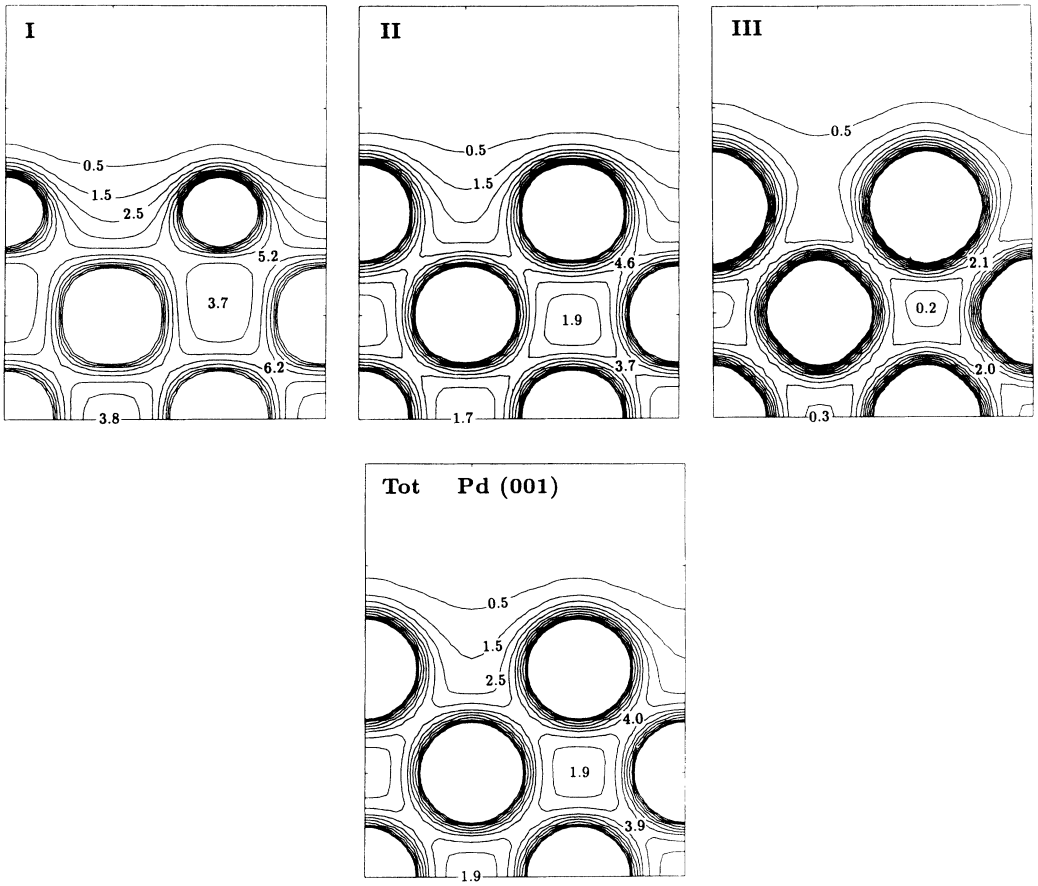

FIG. 11. Charge densities for the Pd(100) surface for the three energy ranges indicated in Fig. 10 and the total density. The densities were normalized to one electron per bulk Pd atom by multiplying with 0.327, 0.276, 0.301 (partial densities), and 0.1 (total). Units are 0.001 Bohr^{-3}.

seen from the unexpectedly large values of σ/E_{coh} for the group-II metals. Good agreement was found to the values of Tyson and Miller, who estimated the solid surface energies from those of the liquid metals. The calculated trends of the top-layer relaxation, including the dependence on the surface roughness, could be understood as an interplay between *sp* smoothing and the effect of localized *d* bonds. The results also suggest that an additional effect, tending to an outward force near the end of the series, could be present. While the calculations give relaxations close to zero for the smoother surfaces of Pd, the experimentally deduced outward relaxation for the Pd(100) surface was not confirmed.

ACKNOWLEDGMENT

We thank S. Weber for assistance in the initial stages of the surface-relaxation calculations.

*Permanent address: Department of Theoretical Physics, Humboldt-University of Berlin, Invalidenstrasse 110, O-1040 Berlin, Germany.

[1]F. Jona and P. M. Marcus, in *The Structure of Surfaces II,* edited by J. F. Van der Veen and M. A. Van Hove, Springer Series in Surface Sciences Vol. 11 (Springer-Verlag, Berlin, 1988), p. 90.

[2]W. Kohn and L. J. Sham, Phys. Rev. **140**, A1133 (1965).

[3]L. Hedin and B. I. Lundqvist, J. Phys. C **4**, 2064 (1971).

[4]K. M. Ho and K. P. Bohnen, Vacuum **41**, 416 (1990).

[5]K. M. Ho and K. P. Bohnen, Phys. Rev. B **32**, 3446 (1985).

[6]D. R. Hamann and P. J. Feibelman, Phys. Rev. B **37**, 3847 (1988).

[7]P. J. Feibelman and D. R. Hamann, Surf. Sci. **234**, 377 (1990).

[8]C. L. Fu, S. Ohnishi, E. Wimmer, and A. J. Freeman, Phys. Rev. Lett. **53**, 675 (1984).

[9]J. Quinn, Y. S. Li, D. Tian, H. Li, F. Jona, and P. M. Marcus, Phys. Rev. B **42**, 11 348 (1990).

[10]W. Oed, B. Dötsch, L. Hammer, K. Heinz, and K. Müller, Surf. Sci. **207**, 55 (1988).

[11]M. Methfessel, Phys. Rev. B **38**, 1537 (1988).

[12]M. Methfessel, C. O. Rodriguez, and O. K. Andersen, Phys. Rev. B **40**, 2009 (1989).

[13]J. P. Perdew and A. Zunger, Phys. Rev. B **23**, 5048 (1981). The spin-polarization energy of the free atoms was obtained from separate calculations of the polarized and nonpolarized free atoms using the exchange-correlation potential of S. H. Vosko, L. Wilk, and M. Nusair, Can. J. Phys. **48**, 1200 (1980).

[14]R. Feder and J. Kirschner, Surf. Sci. **103**, 75 (1981); F. S. Marsh, M. K. Debe, and D. A. King, J. Phys. C **10**, 937 (1977).
[15]C. Kittel, *Introduction to Solid State Physics,* 5th ed. (Wiley, New York, 1976), p. 85.
[16]V. L. Moruzzi, J. F. Janak, and A. R. Williams, *Calculated Electronic Properties of Metals* (Pergamon, New York, 1978).
[17]*CRC Handbook of Chemistry and Physics,* 67th ed., edited by R. C. Weast, M. J. Astle, and W. H. Beyer (CRC, Boca Raton, 1987), p. E-89.
[18]H. B. Michelson, J. Appl. Phys. **48**, 4729 (1977).
[19]G. P. Srivastava and D. Weaire, Adv. Phys. **36**, 463 (1987).
[20]D. McLachlan, Acta. Metall. **5**, 111 (1975).
[21]R. A. Swalin, *Thermodynamics of Solids* (Wiley, New York, 1963).
[22]S. H. Overbury, P. A. Bertrand, and G. A. Somerjai, Chem. Rev. **75**, 547 (1975).
[23]L. Z. Mezey and J. Giber, Jpn. J. Appl. Phys. **21**, 1569 (1982).
[24]A. S. Skapski, J. Chem. Phys. **16**, 389 (1948).
[25]R. A. Oriani, J. Chem. Phys. **18**, 575 (1950).
[26]Reference 23 incorrectly states that the energy for removing an atom from the solid is $C_S\varepsilon$, supposedly because the atom is removed from the surface; this neglects that a new surface atom is created below the removed atom. The incorrect argument directly leads to the empirically found factor of $\frac{1}{6}$.
[27]I. J. Robertson, M. C. Payne, and V. Heine, Europhys. Lett. **15**, 301 (1991).
[28]Liquid-metal densities and heats of vaporization from *Handbook of Chemistry and Physics,* 55th ed., edited by R. C. Weast (CRC, Cleveland, 1974), pp. B-235 and D-56; surface energies are representative values from *ibid.*, 67th ed., p. F-20. The molar surface area was calculated using a geometrical factor of 1.09 for fcc and hcp, 1.12 for bcc, and 1.14 for others (see Ref. 23).
[29]M. Alouani, R. C. Albers, and M. Methfessel, Phys. Rev. **43**, 6500 (1991).
[30]J. H. Rose, J. R. Smith, and J. Ferrante, Phys. Rev. B **28**, 1835 (1983).
[31]W. R. Tyson and W. A. Miller, Surf. Sci. **62**, 267 (1977).
[32]A. R. Miedema, Z. Metallk. **69**, 287 (1978).
[33]F. Cyrot-Lackmann, J. Phys. Chem. Solids **29**, 1235 (1968).
[34]M. Weinert, R. E. Watson, J. W. Davenport, and G. W. Fernando, Phys. Rev. B **39**, 12 585 (1989).
[35]G. J. Ackland and M. W. Finnis, Philos. Mag. A **54**, 301 (1986); G. J. Ackland, G. Tichy, V. Vitek, and M. W. Finnis, *ibid.* A **56**, 735 (1987).
[36]S. M. Foiles, M. I. Baskes, and M. S. Daw, Phys. Rev. B **33**, 7983 (1986).
[37]M. Lannoo and P. Friedel, *Atomic and Electronic Structure of Surfaces* (Springer, Berlin, 1991).
[38]J. R. Smith and A. Banerjea, Phys. Rev. Lett. **59**, 2451 (1987).
[39]J. Perdew, Y. Wang, and E. Engel, Phys. Rev. Lett. **66**, 508 (1991).
[40]E. Krotschek and W. Kohn, Phys. Rev. Lett. **57**, 862 (1986).
[41]N. D. Lang and W. Kohn, Phys. Rev. B **1**, 4555 (1970).
[42]M. W. Finnis and V. Heine, J. Phys. F **4**, L37 (1974).
[43]R. Smoluchowski, Phys. Rev. **60**, 661 (1941).
[44]R. N. Barnett, Uzi Landman, and C. L. Cleveland, Phys. Rev. B **28**, 1685 (1983).
[45]P. Jiang, P. M. Marcus, and F. Jona, Solid State Commun. **59**, 275 (1986).
[46]D. G. Pettifor, J. Phys. F **8**, 219 (1978).
[47]V. Heine and L. D. Marks, Surf. Sci. **165**, 65 (1986).
[48]L. Pauling, J. Amer. Chem. Soc. **53**, 1367 (1931).
[49]A. P. Sutton, M. W. Finnis, D. G. Pettifor, and Y. Ohta, J. Phys. C **21**, 35 (1988).
[50]G. Allan and M. Lannoo, Phys. Rev. B **37**, 2678 (1988).
[51]G. Allan and M. Lannoo, Surf. Sci. **40**, 375 (1973).
[52]G. Allan and M. Lannoo, Phys. Status Solidi B **74**, 409 (1976).
[53]J. Sokolov, F. Jona, and P. M. Marcus, Solid State Commun. **49**, 307 (1984).
[54]R. S. Mulliken, J. Chem. Phys. **23**, 1833 (1955).
[55]D. Spanjaard, C. Guillot, M.-C. Desjonqueres, G. Treglia, and J. Lecante, Surf. Sci. Rep. **5**, 1 (1985).